Wound Repair and Regeneration

WILEY | WHS WOUND HEALING SOCIETY

ORIGINAL ARTICLE-BASIC SCIENCE OPEN ACCESS

Candidate Biomarkers for Hard-to-Heal Wounds Revealed by Single-Cell RNA Sequencing of Wound Fluid in Murine Wound Models

Qi Qin[1] | Daijiro Haba[2] | Chihiro Takizawa[1] | Sanai Tomida[1] | Ai Horinouchi[1] | Mikako Katagiri[3] | Seitaro Nomura[3,4] | Gojiro Nakagami[1,2]

[1]Department of Gerontological Nursing/Wound Care Management, Graduate School of Medicine, The University of Tokyo, Tokyo, Japan | [2]Global Nursing Research Center, Graduate School of Medicine, The University of Tokyo, Tokyo, Japan | [3]Department of Cardiovascular Medicine, The University of Tokyo Hospital, Tokyo, Japan | [4]Department of Frontier Cardiovascular Science, Graduate School of Medicine, The University of Tokyo, Tokyo, Japan

Correspondence: Gojiro Nakagami (gojiron@g.ecc.u-tokyo.ac.jp)

Received: 30 September 2024 | **Revised:** 30 March 2025 | **Accepted:** 23 April 2025

Funding: This study was supported by the Fusion-Oriented Research for Disruptive Science and Technology (FOREST) of the Japan Science and Technology Agency (Grant JPMJFR205H), Japan Society for the Promotion of Science KAKENHI (Grant 23KJ0482, Grant 23H00547) and the Research Support Project for Life Science and Drug Discovery (Basis for Supporting Innovative Drug Discovery and Life Science Research (BINDS)) from AMED (Grant JP23ama121016).

Keywords: hard-to-heal wounds | single-cell analysis | wound dressings | wound fluid | wound healing

ABSTRACT

Wound healing is often hindered by hyperglycemia, chronic inflammation and ageing. Despite extensive research on the pathophysiology of hard-to-heal wounds, wound healing remains complex and poses challenges in treatment and management. Current wound treatments and care mostly target a single pathology, such as infection, while most hard-to-heal wounds are multifactorial. Therefore, exploring the factors that do not rely on a single pathology is crucial to fill the gap in current wound management. Despite containing more comprehensive information than commonly used wound tissue samples, cells in the wound fluid have not drawn much attention because of collection difficulties. This study aimed to use single-cell RNA sequencing (scRNA-seq) of cells from wound fluid to identify specific biomarkers for hard-to-heal wounds, with the hypothesis that common biomarkers among various wound models can be potentially applied to complex hard-to-heal wounds in clinical settings. Three representative delayed wound models, aged, diabetic and lipopolysaccharide-induced inflammatory wound models, were compared with normal young mice to explore commonly shared genes that exist in different pathological delayed wound healing models. The shared upregulation of cell cycle and cellular senescence-related genes such as *Rpl11*, *Rpl26*, *Rps3*, *Rps15*, *Rps 20*, *Rps26*, *Ccl2*, *Cdk2ap2* and *Ccnd3* and the downregulation of immune response regulation genes such as *Tnfaip3*, *Junb*, *Il1r2*, *Plaur*, *Il1rn*, *Il1a*, *Cxcl2*, *Cd14*, *S100a8* and *S100a9* in all delayed healing wound models were found in most immune cell subgroups, especially the macrophage subgroup. The results of this study suggested cellular senescence of cells in wound fluid could be related to hard-to-heal wounds.

Abbreviations: DEG, differentially expressed gene; DFU, diabetic foot ulcer; DGE analysis, differential gene expression analysis; GO enrichment analysis, Gene Ontology enrichment analysis; H&E, haematoxylin and eosin; LPS, lipopolysaccharide; PBS, phosphate-buffered saline; PC, principal component; PCA, principal component analysis; PWD, post-wounding day; RPL, ribosomal protein large subunit; RPS, ribosomal protein small subunit; scRNA-seq, single-cell RNA sequencing; UMAP, uniform manifold approximation and projection; UMI, unique molecular identifier.

This is an open access article under the terms of the Creative Commons Attribution-NonCommercial-NoDerivs License, which permits use and distribution in any medium, provided the original work is properly cited, the use is non-commercial and no modifications or adaptations are made.

© 2025 The Author(s). *Wound Repair and Regeneration* published by Wiley Periodicals LLC on behalf of The Wound Healing Society.

1 | Introduction

Hard-to-heal wounds are wounds that fail to restore the anatomical and functional integrity of the injured site through an orderly and timely repair process [1]. Hard-to-heal wounds are a significant drain on healthcare resources, including equipment and medications, as well as on the valuable time of healthcare professionals [2, 3]. Diabetic foot ulcers (DFUs) and pressure injuries are two major types of hard-to-heal wounds with a low likelihood of healing and long treatment duration. From a healthcare public payer perspective, the mean 1-year cost for managing a DFU is estimated at $44,200 or $15,400 for a pressure injury [4]. The cost of wound care, the loss of productivity and the reduced quality of life for patients and the families who care for them result in tremendous losses to society [3]. Thus, predicting and preventing hard-to-heal wounds is essential for reducing the burden.

Wound healing is a dynamic and complex biological process that can be divided into four partially overlapping phases: haemostasis, inflammation, proliferation and remodelling [5]. In hard-to-heal wounds, many factors may impede the transition from the inflammation to the proliferation phase, consequently delaying wound healing. This highlights the need for prediction, prevention and therapeutic strategies that target this critical phase transition in hard-to-heal wounds [6]. Factors affecting this transition include both systemic and local factors. Systemic factors include diseases such as diabetes, systemic inflammation and vascular impairment, which can act through local effects such as hypoxia, infection or a combination of these [7]. However, while the standard of care includes glucose control-based treatment and interventions for infections and vascular issues, healing can still be hindered by local pathological factors [1, 8]. Therefore, it is essential to elucidate wound local non-healing mechanisms and develop new wound care approaches to evaluate and target these factors at the cellular and molecular levels [6, 9].

Evaluating the wound local environment using molecular techniques holds promise for developing more effective treatment protocols tailored to wound status [10]. The healing phase involves many cell types, including inflammatory cells, fibroblasts, keratinocytes, endothelial cells, growth factors and enzymes [11, 12]. Several different cell types are involved in the wound healing process, and the cellular activities of any particular cell type may vary during various phases of wound repair. Therefore, although many studies have investigated abnormal biomarkers, such as change of C-X-C motif chemokine ligand 5 (CXCL)5 [13], CXCL6 [14] and hypoxia-inducible factor 1-alpha (HIF-1α) [15] to predict the wound healing outcome, adapting them as targets for prevention or treatment is challenging. This difficulty arises primarily because these biomarkers are based on analysing the bulk of cells from different types of cells and cells from different healing phases and represent products of complex and varied cellular pathways [16]. As mentioned above, cellular activities are not concurrent, and gene expression varies among cells of the same cell type. Therefore, the real relationship between delayed wound healing and changes in cellular activity can be masked. Thus, to detect the real relationship and cellular activities, we must detect the activity status of each cell simultaneously and separately. The recently developed single-cell RNA-seq (scRNA-seq) method has the advantage of analysing gene expression at a single-cell level for a population of cells. ScRNA-seq can also be used to detect cell-specific changes in transcription and to analyse cell subtypes. This will be able to provide a better understanding of the relationship of each cell's activity changes and wound healing [17]. ScRNA-seq provides the possibility of detecting more specific predictive biomarkers with higher prediction accuracy as well as targets for tailored treatment [18].

Several recent studies have focused on identifying dysregulated gene expression during delayed wound healing using scRNA-seq [19–22]. However, these studies primarily utilised invasive sample types, such as tissue biopsy, debridement or blood samples. The gene expression profiles obtained from these samples may be biased and highly dependent on the technique used and the specific area of tissue collected [22]. In contrast, the present study focused on wound fluid, which offers a rich and well-distributed array of information about wounds and has the distinctive advantage of enabling non-invasive, continuous evaluation [23]. Wound fluid encompasses a diverse range of proteins and inflammatory components that reflect changes in the wound environment. It also contains numerous functional cells, including inflammatory cells, keratinocytes and fibroblasts, all of which play crucial roles in the wound healing process [24, 25]. Although cellular activities in wound tissues have been well documented, the functions and changes of cells in the wound fluid have not been well studied. Our research group has developed a novel method to collect cells from discarded wound dressings without altering their gene expression [26]. This enabled the investigation of gene expression in wound fluid. Utilising scRNA-seq to investigate cells in wound fluid can reveal additional underlying mechanisms of hard-to-heal DFUs.

This study aimed to identify shared biomarkers across various pathological wound models that are specific to hard-to-heal wounds. This study was designed to utilise different delayed wound healing models to investigate shared biomarkers across various pathological hard-to-heal wounds. Such biomarkers, if identified, could potentially be applied for all types of hard-to-heal wounds. By focusing on scRNA-seq of cells in wound fluid, the study sought to uncover molecular mechanisms underlying delayed wound healing. Furthermore, it provides information on candidates that could be potentially used to predict and potentially serve as therapeutic targets for hard-to-heal wounds.

2 | Materials and Methods

2.1 | Animals and Ethics

All mice were purchased from the Jackson Laboratory Japan (Kanagawa, Japan) and kept in the university animal building under specific pathogen-free conditions with a temperature of 23°C ± 2°C, humidity of 45% ± 10%, 12:12 h light–dark cycle, and ad libitum feeding and drinking. The experimental protocols for this study were approved by the Animal Research Committee of the University of Tokyo (P21-095) and were conducted in accordance with the National and International Guidelines for Animal Welfare, including the Guide for the Care and Use of Laboratory Animals issued by the National Institutes of Health.

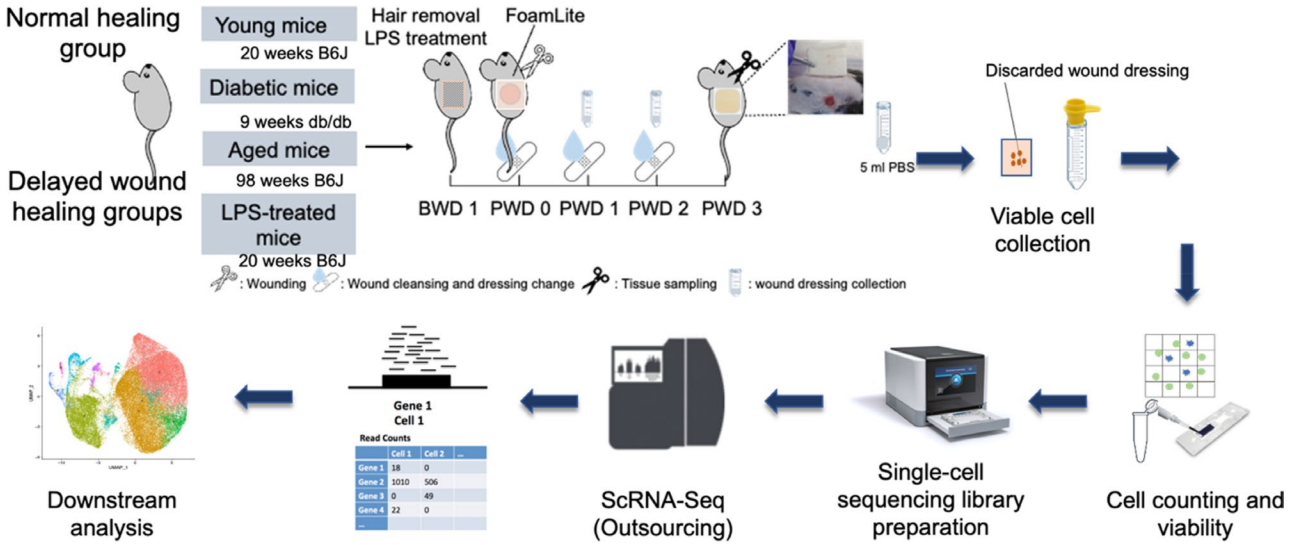

FIGURE 1 | Abbreviated methods for scRNA-seq workflow. Upper procedures are procedures for obtaining cells from discarded wound dressings. Down procedures are scRNA-seq workflows.

2.2 | Delayed Wound Healing Models

Four groups were established to represent different wound healing types, including three well-established models of delayed wound healing: db/db mice (hyperglycemia/diabetic model) [27], lipopolysaccharide (LPS)-induced inflammation model [28], 98-week-old mice (ageing model) [29] and one normal healing group (Figure 1). Eight 20-week-old male C57BL/6J mice, four 9-week-old male db/db (*BKS.Cg-Dock7m +/+ Lepr^{db}/J*) mice, and four 98-week-old male C57BL/6J mice were used as full-thickness wound models. Twenty-week-old mice were used because of the large weight differences between the young (9-week-old) normal, LPS, aged and diabetic groups, which significantly affected wound healing in our preliminary studies. To make an LPS-induced inflammation model, at 24 and 2 h before wound creation, four healthy 20-week-old male C57BL/6J mice received 10 μg LPS in 1 mL phosphate-buffered saline (PBS) injection on the wound site subcutaneously [28]. LPS derived from *Klebsiella pneumoniae* (Sigma Aldrich, St. Louis, MO) was used. A 1.5-cm diameter full-thickness wound was created on the left side of the abdomen using sterilised scissors for each mouse under anaesthesia (Isoflurane inhalation, 2%, 0.2 L/min; Pfizer, Tokyo, Japan). The centre of the wound was located on the lateral midline between the middle of the greater trochanter and the axilla. Silicone-faced foam dressings (FoamLite, ConvaTec Japan Co. Ltd., Tokyo, Japan) were used to cover the wounds. From the first post-wounding day (PWD1) to PWD2, the wounds were rinsed daily with saline, and wound dressings were changed. Wound images were captured daily, and wound size was measured using ImageJ software ver. 1.53i (National Institutes of Health, Bethesda, MD). The wound dressings on PWD3 were collected and placed in 5 mL PBS for cell collection. The critical part of wound healing is whether the wound can successfully transition from the inflammatory phase to the proliferation phase; therefore, preliminary experiments were conducted to confirm which day all delayed wound healing models showed significant differences compared to that of the normal healing group. As a result, all groups had significantly larger relative wound sizes on PWD4; thus, PWD3 was considered the start of the wound healing process and was set as the sampling day. Cells were collected using the methods previously established [26]. The wound tissue was sampled under anaesthesia, immersed in 10% formalin (FUJIFILM Wako Pure Chemical Corporation) for 24 h, and then used for histological analysis (haematoxylin and eosin [H&E] staining) to confirm the healing phase. After sampling, the mice were sacrificed using CO_2 gas.

2.3 | ScRNA-Sequencing Library Preparation

After using a 40-μm Flowmi Cell Strainer (Sigma–Aldrich) to remove the debris and multiplets, 7000 cells were prepared to a concentration of 1000 cells/μL and loaded into the Chromium Controller (10× Genomics, Pleasanton, CA), and single-cell cDNA libraries were generated using the Chromium Next GEM Single Cell 3′ Reagent Kits v3.1 (10× Genomics, PN-1000269) according to the manufacturer's instructions. Libraries were sequenced on a NovaSeq 6000 system (Illumina, San Diego, CA) using a NovaSeq S4 reagent kit (200 cycles; 20027466; Illumina) (Figure 1).

2.4 | ScRNA-Seq Data Processing

Raw data was generated from RNA-seq. Base calls from the raw FASTQ files of each sample were processed using the Cell Ranger count pipeline (10× Genomics, version 7.1) using 10× Genomic Cloud Analysis [30]. The Cell Ranger count pipeline outputs a web summary file describing sequencing quality and a feature-barcode matrix containing gene expression counts and feature barcode counts for each barcode. Cell Ranger mm10 genome was used as a reference. Subsequent data processing used these raw counts as input and was performed using the Seurat R package (version 4.3.0.1) [31],

employing the specific functions detailed below. Quality control metrics, including the distribution of genes and unique molecular identifier (UMI) counts per cell, were assessed prior to normalisation. Specifically, cells with fewer than 1000 and more than 2000 detected genes were considered empty drops, and doublets were excluded. Cells with mitochondrial gene content exceeding 5% of the total UMI were excluded. After filtering, read counts were normalised with the 'NormalizeData' function (using a default scale factor of 10,000) on an individual dataset basis. Two samples were processed on different days; therefore, batch effects were corrected using the 'Harmony' integration method. Two datasets were harmonised through the 'FindIntegrationAnchors' and 'IntegrateData' functions. Dimensionality reduction and clustering were performed using the integrated data. UMI counts were normalised using 'SCTransform', while principal component analysis (PCA) was achieved through the 'RunPCA' function. The 'FindNeighbors' function identified nearest neighbours for each single-cell data point, and the optimal number of principal components (PCs) was determined using an elbow plot. PCs established the graph-based clustering into specific cell populations with the 'FindClusters' function, with the resolution parameter adjusted based on clustree analysis. To visualise single-cell location on a two-dimensional plot, we employed the uniform manifold approximation and projection (UMAP) method, projecting cells into a two-dimensional space using the 'RunUMAP' function. 'FindAllMarkers' function was then used for identifying top features of each cluster, for later use of annotation cell types of each cluster. To identify differentially expressed genes (DEGs) in each hard-to-heal group compared to the normal group, criteria were set at a $|\log_2 FC| > 0.25$ and an adjusted $p < 0.05$, using the 'FindMarkers' function for differential gene expression (DGE) analysis. Gene Ontology (GO) enrichment analysis was used to identify the biological process of shared common genes in each subcluster using the 'clusterProfiler' package with reference 'org.Mm.eg.db'. Clusters were manually labelled using the top 100 features of each cluster identified by 'FindAllMarkers' function, based on the expression of known marker genes and comparison with reference datasets provided by GO enrichment analysis, PanglaoDB, CellMarker 2.0 and annotations from 'scCATCH' [32–34]. The subset cell clusters were then normalised and reduced dimension through a series of Seurat functions: 'ScaleData', 'RunPCA', 'FindClusters', 'RunUMAP' and 'FindMarkers'. To identify DEGs, each group classified as 'hard-to-heal' was compared with the normal group. Subsequently, shared dysregulated biomarkers among each cell subgroup were determined. Shared dysregulated biomarkers across the hard-to-heal groups were visualised using a Venn diagram.

2.5 | Histological Analyses

All the harvested tissues were fixed overnight in 10% neutral-buffered formalin at room temperature (25°C), dehydrated in a series of ethanol and xylene substitutes, G-Nox (Genostaff, Tokyo, Japan) and embedded in paraffin. The paraffin-embedded tissues were sectioned at 3-μm thickness for H&E staining.

2.6 | Statistical Analysis

Wound size from PWD1 to PWD3 was compared among the four groups using analysis of variance, and a post hoc analysis was conducted using Tukey's honest significance test. $p < 0.05$ was considered to be statistically significant.

3 | Results

3.1 | Wound Healing Process

Figure 2 shows the differences in wound size among the diabetic, aged and LPS groups from PWD1 to PWD3. On PWD2, both the diabetic and aged groups had significantly larger wound areas compared to the normal group ($p < 0.05$, ANOVA, Tukey's HSD). On PWD3, the diabetic group continued to show a statistically significant difference in wound area compared to that of the normal group ($p < 0.05$, ANOVA, Tukey HSD).

3.2 | ScRNA-Seq Data Process and Results

To analyse wound healing at the cellular level, we performed scRNA-seq on two samples per group: the most delayed healing and most healed wound within each condition. Eight samples were processed, with the estimated number of cells varying among the groups: 29,199 in the aged group, 7628 in the diabetic group, 16,221 in the LPS group and 5523 in the normal group. The mean number of reads per cell exceeded 20,000 in each sample. Sequencing metrics showed that the percentage of valid barcodes was over 97% in every sample, reads mapped to the genome were over 90%, reads mapped confidently to the transcriptome were over 70% and the overall fraction of reads in the cells was over 90%. The median number of genes across all samples was approximately 1500, although there were variations among different groups. We aimed to process 7000 cells in each group; however, the number of processed cells varied among the groups. After removing potential empty droplets, doublets and cells with high mitochondria (mitochondria percentage < 5%), the number of cells in each group used in the data analyses were as follows: 6997, 3052, 8130 and 4080 in the aged, diabetic, LPS and normal groups, respectively.

3.3 | Cell Clustering and Annotation

The cell clustering and annotation processes used in this study are shown in Figure 3. We identified nine main cell types in wound fluid. The top-expressed genes in each cell cluster were used for cluster annotation. Cluster 0 was annotated as a macrophage because of the high expression levels of *Lyz2*, *Adgre1* (F4/80) and *Cd14*, which are known markers of this cell type. Cluster 1 cells showed significant expression of *Cd275* and *Basp1*, leading to their identification as dendritic cells. T cells were identified in Cluster 2, as indicated by the expression of genes such as *Stk10*, *Nr4a1*, *Ikzf1* and *Adgre5*. Cluster 3 monocytes exhibited high levels of *Ptgs2*, *Entpd1* and *Il1b1*. Fibroblasts were identified in Cluster 4 based on the expression of *Fn1*, *Sdc4* and *Vim*. Cluster 5, with prominent

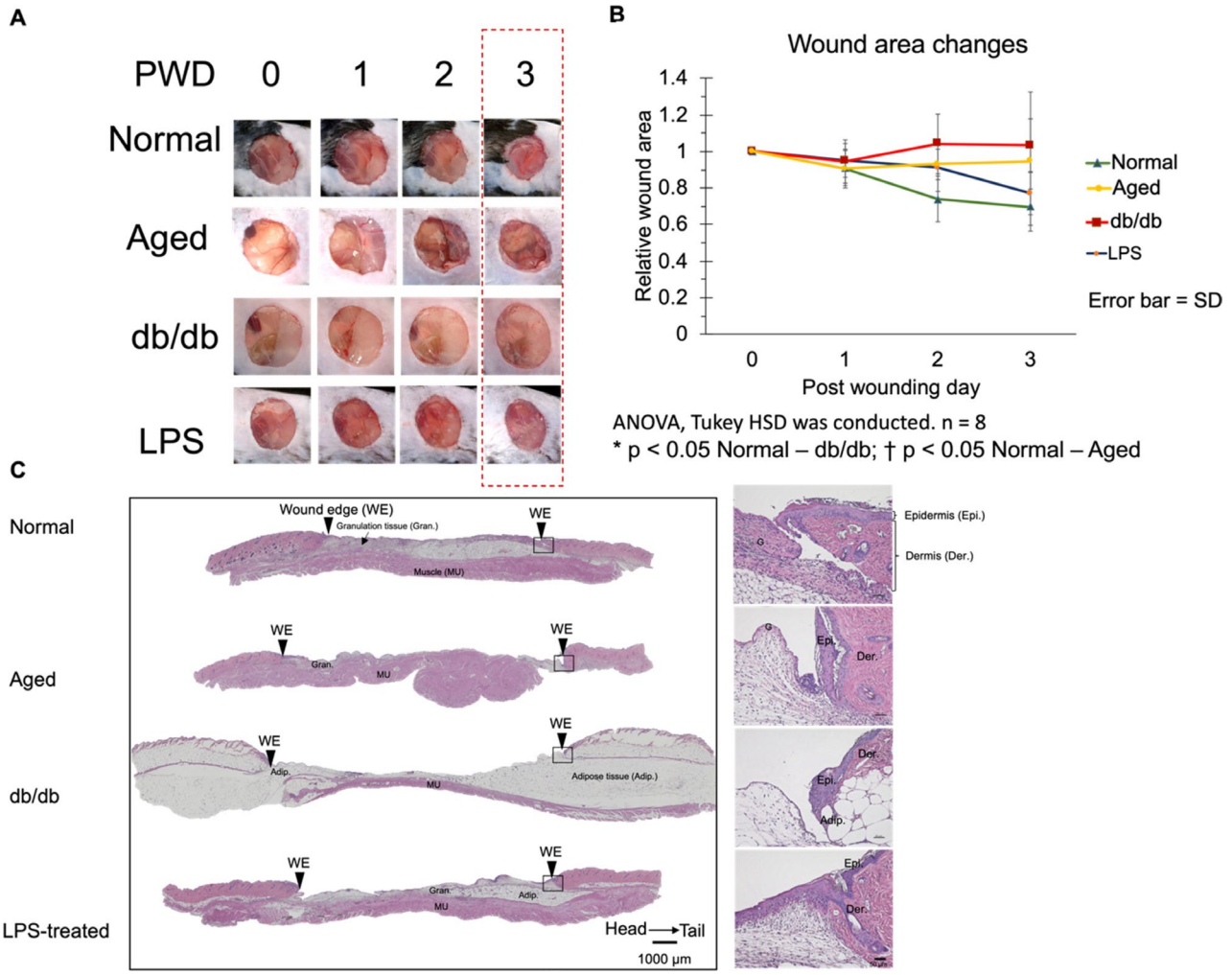

FIGURE 2 | Wound healing process. (A) Representative macroscopic images of wounds from PWD0 to PWD3. PWD: post-wounding day. (B) Relative wound area changes from PWD0 to PWD3. $n = 8$; data are presented as mean ± SD. Statistical analysis was performed using ANOVA followed by Tukey's HSD test. $^{*}p < 0.05$ normal versus diabetic, $^{\dagger}p < 0.05$ normal versus aged. (C) Histological analysis of selected samples on PWD3. The left panel presents 4× magnification images providing an overview of the wounds, while the right panel displays 20× magnification images focusing on the right wound edge. Adipose tissue (Adip.), dermis (Der.), epidermis (Epi.), granulation tissue (Gran.), muscle (MU), and wound edge (WE) are labelled. Left panel scale bar = 1000 μm, right panel scale bar = 50 μm.

expression of *Lcn2*, was annotated as neutrophils. Cluster 6 showed expression of *Ly6a* and *Ly6g*, which led to their annotation as stem cells. Erythroid terminal differential cells were identified in Cluster 7 owing to the high expression of *Car2*, *Hba-a1*, *Hba-a2* and *Hbb-bs*. Finally, Cluster 8 was annotated as endothelial based on the expression of Pecam1, a known marker of endothelial cells (Figure 3E).

3.4 | Cell Type and Cell Proportion in Each Wound Healing Group

Figure 4 presents various aspects of cell cluster distribution across different groups in this study. UMAP showed the distribution of cell clusters in each group, revealing variations in the fibroblast cell clusters among the four groups (Figure 4A). Panel B of Figure 4 provides insights into the cell types present in the wound fluid at PWD3. The three most prevalent cell types were macrophages, dendritic cells and T cells. Figure 4C shows the cell proportions in each wound healing group, noting large differences, particularly in the fibroblasts, erythroid terminal differential cells and endothelial cells, when comparing the delayed wound healing groups to the normal healing group.

3.5 | Shared Dysregulated Genes in Each Cell Subgroup

To identify common patterns in delayed wound healing, we examined DEGs (DEG analysis, $|\mathrm{Log_2FC}| > 0.25$, adjusted $p < 0.05$) that were shared, upregulated or downregulated across the diabetic, aged and LPS-treated groups (Figures 5 and 6, Table S1, Figures S1–S7).

In macrophages, 254 genes were upregulated and 888 were downregulated, with enrichment in ribosomal activity and immune suppression pathways (Figure 5). Dendritic cells, T cells and monocytes exhibited similar patterns of increased protein synthesis-related genes and reduced immune-related gene expression (Figures S1–S3).

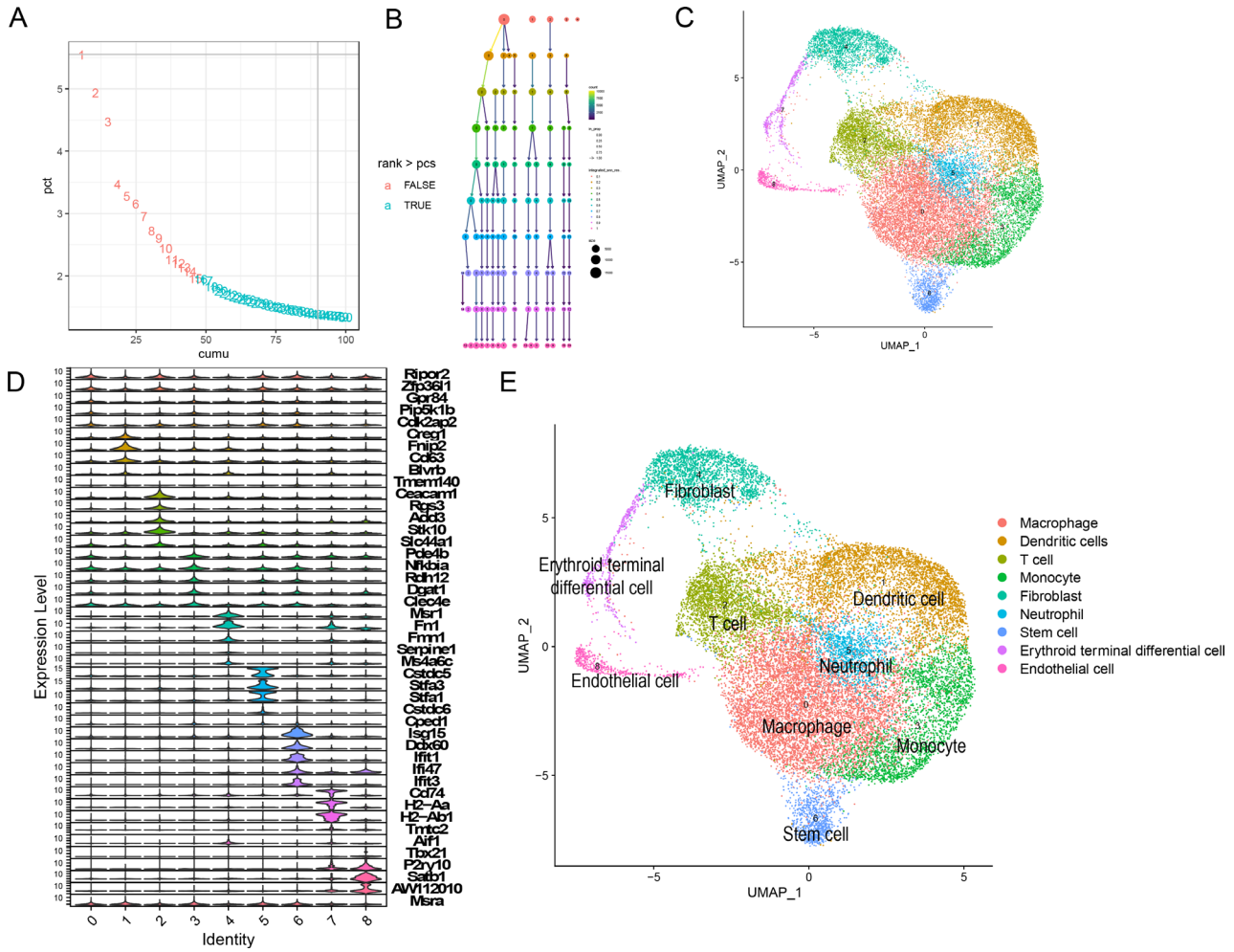

FIGURE 3 | Clustering and cell annotation. (A) The elbow plot was used to determine the optimal number of principal components. The elbow corresponds to the point where the red-coloured and green-coloured numbers connect, indicating 15 as the optimal number of principal components. (B) Clustree for determining resolution in dimension reduction. The Clustree shows the number of cluster changes and the stability of clusters at different resolutions. Each colour represents a different resolution, ranging from 0.1 (top lane, coloured in orange) to 1.0 (bottom lane, coloured in purple). Resolution 0.4 (fourth lane, coloured in green) was considered optimal as the clusters are most stable at this resolution. (C) UMAP embedding of 22,259 single-cell expression profiles from eight mice ($n = 2$ for each group). Each dot represents one cell, and each colour indicates one cell cluster. (D) Stacked violin plot showing the top five highly expressed genes for each cluster compared to others (DGE analysis, log2FC > 0.25, adjusted $p < 0.05$). The *x*-axis shows the cluster number, and the *y*-axis shows the top genes in each cluster. (E) Cell clusters were manually annotated based on the top genes expressed in each cluster. Clusters 0–8 were identified as macrophages, dendritic cells, T cells, monocytes, fibroblasts, neutrophils, stem cells, erythroid terminal differentiation cells and endothelial cells, respectively.

Fibroblasts showed a distinct profile, with only one upregulated gene (*Lyz2*) and 92 downregulated genes, primarily linked to an aggressive defence response to bacteria, and suppressed inflammatory signalling (Figure 6). Neutrophils, stem cells, erythroid cells and endothelial cells displayed consistent downregulation of immune response pathways (Figures S4–S7).

A complete list of shared dysregulated genes across cell types is provided in File S1. Among immune cell types, 126 genes were consistently downregulated, including key immune response genes (*Il1rn*, *Cxcl3*, *Cxcl2*, *Junb*, *Tnfaip3*, *Tnfaip2*, *Nfkb2*, *Il1a*, *Il1b*, *Cd14*, *S100a8* and *S100a9*) and anoikis-related genes (*Bcl3*, *Cebpb*, *Macl1*, *Thbs1*, *Ptgs2*, *Plaur*, *Fas*, *Cflar* and *Sbdbp*). Due to the lower number of differentially expressed genes in adherent cells, no genes were shared across fibroblast, endothelial or erythroid cell clusters. Among shared upregulated genes, a large proportion belonged to ribosomal protein large/small subunits (RPL/RPS), *Rpl6*, *Rpl7*, *Rps25*, *Rplp1*, *Ppia*, *Rps11*, *Rps14*, *Rps6*, *Rps3*, *Rpl27*, *Rpl26*, *Rpl21* and *Rpl29*, as well as *Tgfbi*, *Rbm3*, *Cdk2ap2*, *Rpl35a*, *Cst3*, *S100a10*, *Tmem59*, *Ncl* and *Bag1*. These were particularly enriched in macrophages, dendritic cells and T cells. Additionally, *Ccl2*, *Vim*, *S100a4* and *Zfp36l2* were commonly upregulated in immune cell groups, while *Lyz2* was shared between immune cells and fibroblasts.

4 | Discussion

The current study is the first to use scRNA-seq on cells collected from discarded wound dressings, focusing on three distinct wound healing models: aged, diabetic and LPS-treated groups. These models were selected to represent the primary factors contributing to hard-to-heal DFUs, namely cellular senescence, hyperglycemia and prolonged inflammation [1, 11]. Our results

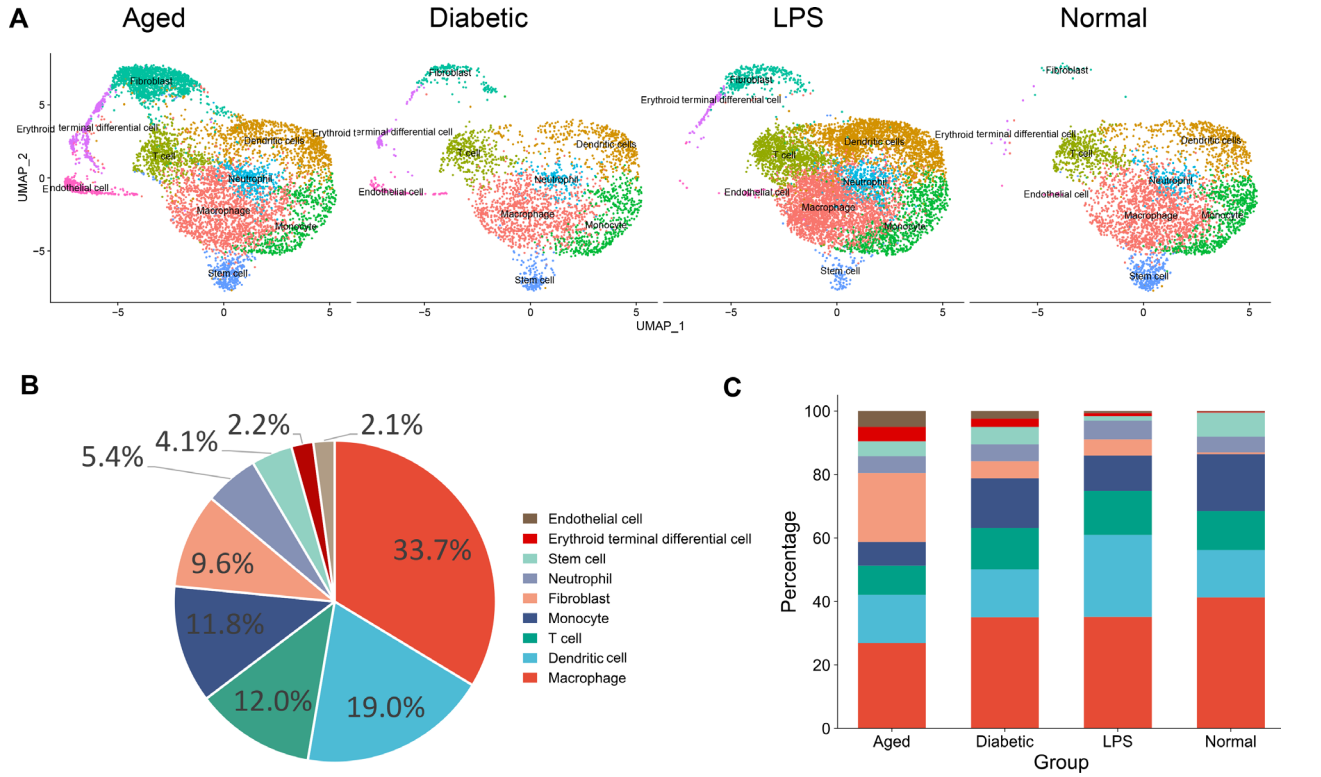

FIGURE 4 | Cell distribution and cell proportion in each group. (A) Cluster differences among four wound healing groups: aged, diabetic, LPS and normal. (B) Overall proportion of cell types in wound fluid. (C) Cell proportion in each of the four wound healing groups.

revealed a variety of cell types in the wound fluid and identified common biomarkers across different types of hard-to-heal wounds within specific cell subgroups. Although the relationship between dysregulation of these genes and wound healing needs to be further investigated, this innovation may be used as predictive biomarkers to enhance the targeting of therapies for hard-to-heal wounds by focusing on the underlying biological mechanisms.

Using cells collected from wound dressings for scRNA-seq is challenging because of the low cell count in the wound fluid and low cell viability. In the present study, the proportion of viable cells collected from the wound dressings was more than 70% (data not shown). Although the number of cells varied in different samples, the number of cells used in the bioinformatics analysis was over 3000. The mean number of reads per cell exceeded 20,000 for every sample, indicating sufficient sequencing depth for reliable downstream analysis. Sequencing quality metrics showed that the percentage of valid barcodes was over 97% in every sample, which was well above the recommended threshold of 80%, indicating minimal technical artefacts. The number of reads mapped to the genome exceeded 90%, surpassing the recommended level of 70%, suggesting high-quality sequencing and alignment. Additionally, over 70% of the reads were confidently mapped to the transcriptome, meeting the standard benchmark for accurate transcript quantification. The overall fraction of reads in the cells was over 90%, which was significantly higher than the recommended 70%, implying a low level of ambient RNA contamination. These high-quality metrics collectively demonstrate that the scRNA-seq data are robust and reliable. After dimension reduction, the cell clusters were well-separated based on the top features, with immune cell clusters, fibroblasts and endothelial cells distinctly segregated in UMAP. The above information suggests that scRNA-seq of cells from the wound dressings was successfully performed.

As the first scRNA-seq was conducted using cells collected from wound dressings, we were able to reveal the cell types in the wound fluid, which are mostly immune cells, fibroblasts and endothelial cells. Immune cells constitute the majority of the cell population in the wound fluid, which has been well documented in previous studies [23, 35, 36]. Adherent cells, including fibroblasts, were identified in this study, corroborating findings from our earlier research that characterised the cell composition in wound fluid [26]. The presence of fibroblasts is consistent with previous observations. However, differences in sampling day PWD3 in the current study versus PWD5 in the previous study may explain why keratinocytes were not detected in the cell population in the current study. This discrepancy suggests that sampling timing can influence the detection of specific cell types in the wound fluid, and the cell types detected in the current study only represent the cell population in the transition period from the inflammatory phase to the proliferation phase. A big difference in the proportion of fibroblasts in wound fluid was observed between the normal healing and delayed healing groups. This phenomenon has not yet been well reported or explained by previous studies. As a possible explanation, fibroblasts in the wound fluid and wound area primarily originate from the surrounding connective tissue or are recruited from circulating precursors. As they migrate to and proliferate within the wound area, some cells might slough off into the wound exudate. Additionally, cellular debris from these cells can be found in the fluid due to cell death, which is common in the dynamic and sometimes hostile environment of a healing

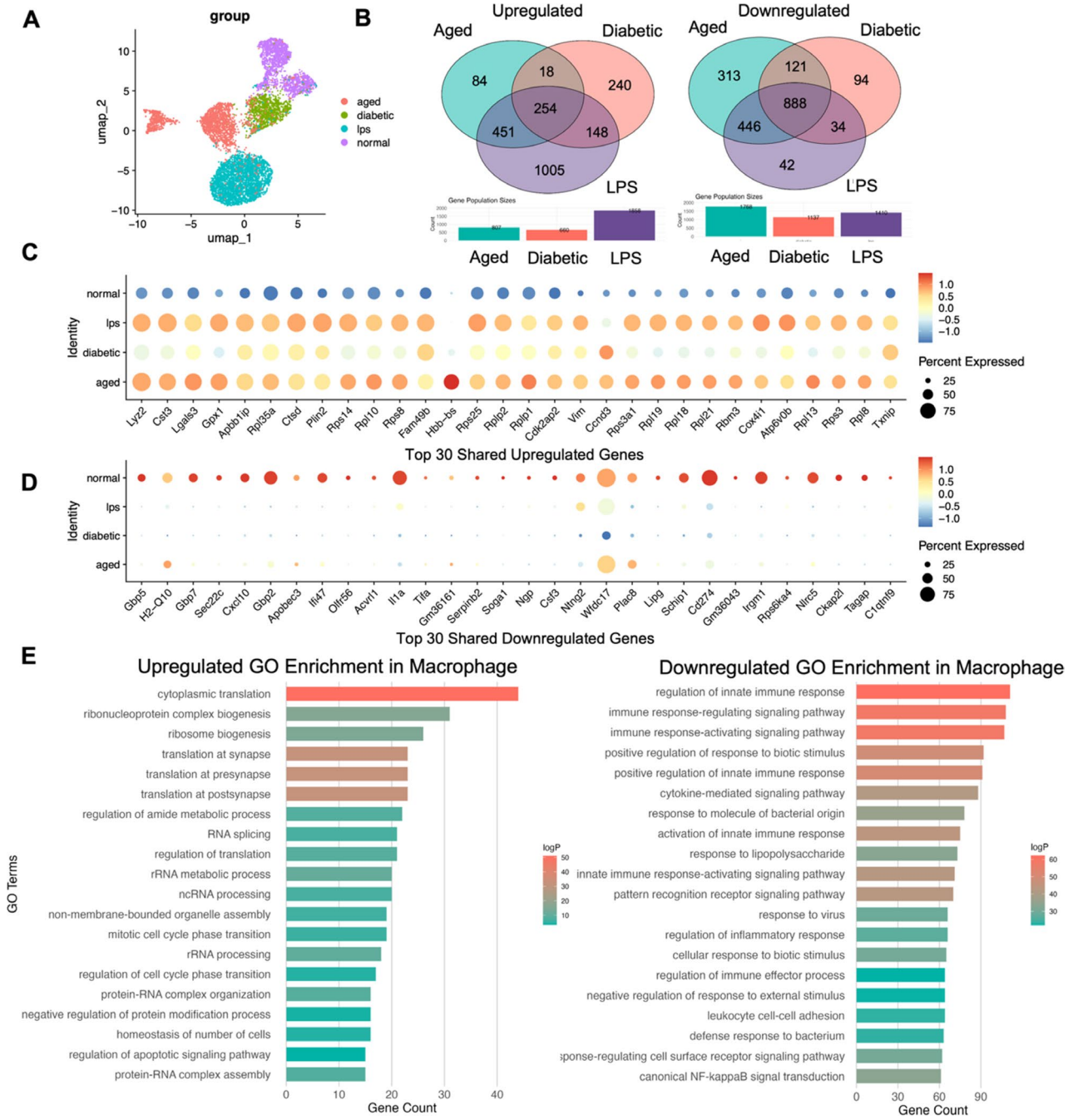

FIGURE 5 | Shared dysregulated genes in macrophage. (A) UMAP of the macrophage subgroup shows the distribution of cells in each group. (B) Shared dysregulated genes among three delayed wound healing groups. The left Venn diagram shows shared upregulated genes, and the right one shows downregulated genes (DGE analysis, $|\log2FC| > 0.25$, adjusted $p < 0.05$, $PC > 0.1$). The middle overlapping area is the gene number shared among three delayed wound healing groups compared to the normal healing group. A total of 254 genes were upregulated and 888 were downregulated. (C) Dot plot of top 30 shared upregulated genes. Top upregulated and downregulated genes were selected based on pairwise differential expression analysis between two groups. The dot plot represents the mean expression levels across all groups, which may result in differences between statistical comparisons and visual representation. (D) Dot plot of top 30 shared downregulated genes. The colour indicates the expression level and the size of the dots indicates the percentage of cells expressing the genes. Blue represents low expression and orange represents high expression. Small dots indicate a low percentage of expressing cells and large dots indicate a high percentage of expressing cells. (E) GO enrichment analysis for dysregulated genes (left: upregulated, right: downregulated). GO enrichment analysis for dysregulated genes (left: upregulated, right: downregulated). GO terms are ordered by gene count and the bar colour indicates −log10 (*p* value), showing the significance of the GO terms. The top upregulated GO terms were cytoplasmic translation, ribonucleoprotein complex biogenesis and ribosome biogenesis owing to the large proportion of ribosomal protein large/small subunit (RPL/RPS) genes. The top three downregulated GO terms were regulation of the innate immune response, immune response-regulating signalling pathway and immune response-activating signalling pathway.

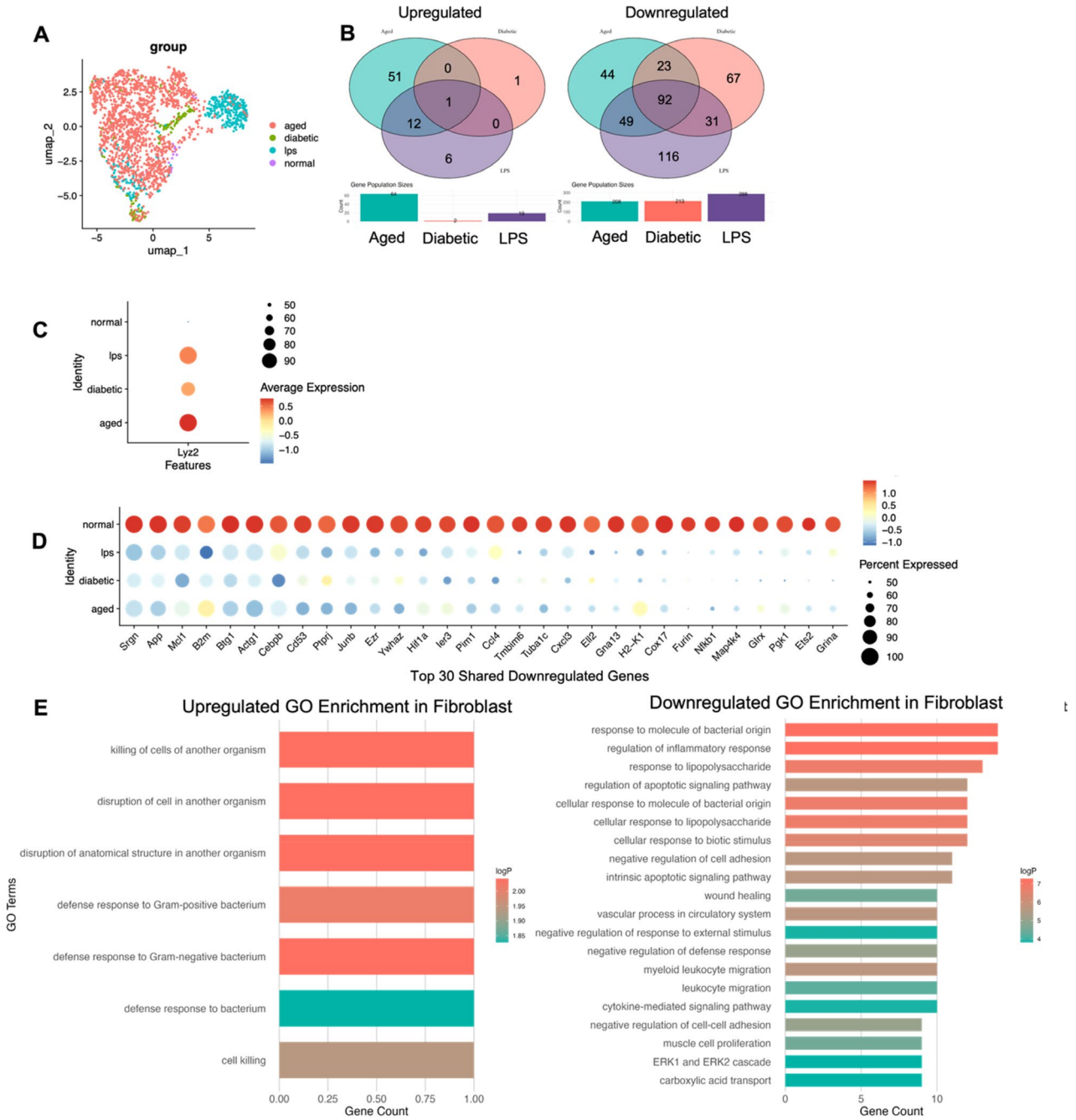

FIGURE 6 | Shared dysregulated genes in fibroblasts. (A) UMAP of fibroblast subgroup shows the distribution of cells in each group. (B) Shared dysregulated genes among three delayed wound healing groups. The left Venn diagram shows shared upregulated genes and the right one shows downregulated genes (DGE analysis, $|\log2FC| > 0.25$, adjusted $p < 0.05$, $PC > 0.1$). The middle overlapping area represents genes shared among three delayed wound healing groups compared to the normal group. (C) Dot plot of the only shared upregulated gene: *Lyz2*. Top upregulated and downregulated genes were selected based on pairwise differential expression analysis between two groups. The dot plot represents the mean expression levels across all groups, which may result in differences between statistical comparisons and visual representation. (D) Dot plot of top 30 most downregulated genes. The colour indicates the expression level and the size of the dots indicates the percentage of cells expressing the genes. Blue represents low expression and orange represents high expression. Small dots indicate a low percentage of expressing cells and large dots indicate a high percentage of expressing cells. (E) GO analysis for dysregulated genes (left: upregulated, right: downregulated). GO analysis for dysregulated genes (left: upregulated, right: downregulated). GO terms are ordered by gene count and bar colour indicates −log10 (*p* value), showing the significance of the GO terms.

wound. Fibroblasts in delayed healing wounds may undergo increased rates of apoptosis or necrosis due to factors such as oxidative stress, high glucose levels and persistent inflammation that can damage fibroblasts, causing them to detach from the extracellular matrix and appear in the wound fluid [12]. This increased turnover of fibroblasts contributes to their elevated presence in the wound fluid. The cell populations detected in the present study were similar, but not exactly the same as those

in other studies that used debrided tissue for scRNA-seq [19, 22]. This difference can be explained by cells from the wound fluid, mostly from capillary leakage; therefore, cell types are expected to differ from those in the wound tissue.

Common upregulated and downregulated genes in the three hard-to-heal wound models were identified. Many genes upregulated in immune cell clusters, including macrophages, dendritic cells, T cells and monocytes, were RPL/RPS genes. Upregulated ribosomal protein genes in immune cell clusters include the following known to be related to the p53 pathway, including *Rpl11*, *Rpl26*, *Rps3*, *Rps15*, *Rps 20* and *Rps26* [37, 38]. GO terms such as cytoplasmic translation, ribonucleoprotein complex biogenesis, ribosome biogenesis and rRNA metabolic process were mostly upregulated in the hard-to-heal wound group, which could also imply high activity of protein synthesis, possibly for cell signalling and repair, which could be a response to cellular stress (GO term: cellular response to oxidative stress), damage and an attempt to repair and regenerate tissues, which can also be indicative of cellular senescence. This finding aligns with a previous study that found that ribosomal proteins, RPS3A and S24, were also presumptively under-expressed in healing foetal wounds, which usually heal rapidly [39]. The ribosomal protein RPL29 has been identified as a biomarker of cellular senescence owing to its accumulation in the nucleoli of various types of senescent cells, including *Ras* oncogene activation-senescent, promyelocytic leukaemia protein-senescent and naturally aged. However, RPL29 does not accumulate in cells that are growth-arrested due to serum starvation or high cell density (confluence), as reported in a previous study [40]. Ribosome biogenesis is linked to senescence, supporting the idea that high ribosomal activity may indicate cellular stress and senescence in delayed wound healing. In addition to ribosomal protein genes involved in cellular senescence, cell cycle-associated genes, such as *Ccl2*, *Cdk2ap2*, *Ccnd3* and *Txnip* were also upregulated [41–43]. Notably, *Ccl2* (monocyte chemoattractant protein-1) is known for recruiting macrophages to the wound sites and promoting cell migration and angiogenesis in the early inflammatory phase [41]. In the current study, *Ccl2* was upregulated on PWD3, and the extensive recruitment of macrophages may be a sign of prolonged inflammation. *Ccnds*, also known as cyclin D3, are essential for the transition from the G1 phase to the S phase of the cell cycle, promoting cell proliferation. During wound healing, its upregulation facilitates the proliferation of keratinocytes and fibroblasts, which are crucial for tissue repair and regeneration. However, we observed an upregulation of *Ccnd3* in the groups with delayed wound healing. This suggests a complex role for *Ccnd3*, as its upregulation in the delayed healing group may indicate dysregulated cell cycle progression or cellular stress responses. *Ccnd3* regulates cell cycle progression by interacting with cyclin-dependent kinases and its dysregulation contributes to cellular senescence [43]. *Txnip* is known to regulate cellular senescence under a glucose-derived oxidative stress response by inhibiting the AKT pathway; upregulation could be a response to high expression of cellular senescence [44]. The effects of cell senescence on wound healing are well documented [45, 46]. The present study identified key biomarkers linked to cellular senescence in wound fluid, shedding light on how these factors contribute to impaired wound healing. These findings could help in developing advanced wound dressings that detect senescence-related risk factors, improving early diagnosis and treatment strategies for hard-to-heal wounds. Additionally, targeting these senescence-associated genes in wound fluid may offer a promising way to promote healing. By pinpointing specific cell subpopulations that show signs of senescence, our study also provides useful guidance for future in vitro research, helping researchers choose the cell types for modelling wound healing and testing potential interventions more effectively.

Downregulated genes in immune cell clusters are mostly involved in immune responses or the control of inflammation-related activities. The most downregulated genes were *Hdc*, *Tnfaip3*, *Junb*, *Il1r2*, *Plaur*, *Il1rn*, *Il1a*, *Cxcl2*, *Cd14*, *S100a8* and *S100a9*. The gene *Tnfaip3* encodes A20, which is one of the negative regulators of the TNF-induced NF-κB pathway. A20-deficient mice die prematurely of multiorgan inflammation, as a result of excessive Toll-like receptor signalling was reported in previous studies. Downregulation in delayed wound healing models can lead to an increased inflammatory state [45, 47]. The reduced expression of *Cxcl2* and S100 protein genes (*S100a8* and *S100a9*) suggests that impaired chemotactic signalling is necessary for neutrophil recruitment, which is essential in the early phases of wound healing [41, 48]. The biological role of S100a8/S100a9 depends on the cell type and wound healing phase [48, 49]. Increased levels of S100A8/S100A9 in neutrophils, monocytes and macrophages during the early inflammatory phase enhance the production of inflammatory mediators, support phagocytosis and oxidative bursts, and enable migration through the epithelium, thereby inducing an inflammatory state. Downregulation of S100a8 and S100a9 may indicate an inadequate inflammatory response leading to prolonged inflammation. The overall downregulation of these genes indicated a compromised immune response and disrupted inflammatory processes, which are crucial for effective wound healing.

There were limited shared dysregulated genes among the fibroblast clusters. We observed the downregulation of *Ccl4*, *Cxcl3*, *Cd53* and *Cebpb* in fibroblast cell clusters. These findings suggest an impaired inflammatory response and reduced immune cell recruitment, both of which are critical for effective wound healing. Previous studies have shown that fibroblasts play an active role in inflammation and tissue repair by producing chemokines, such as *Ccl4* and *Cxcl3*, which recruit macrophages and neutrophils to the wound site. These chemokines are essential in the initial inflammatory phase of wound healing, where they help clear debris and prevent infections [41]. The downregulation of these chemokines in our study aligns with observations in chronic wounds and diabetic conditions, where an impaired inflammatory response is expected. Additionally, *Cd53*'s involvement in immune cell adhesion and migration and *Cebpb*'s role in regulating pro-inflammatory cytokines and growth factors further highlight the importance of these genes in wound healing [50, 51]. In wound healing, pro-inflammatory cytokines, such as IL-6, TNF-α and IL-1β, activate C/EBPβ in macrophages, which in turn activate these cytokines to regulate inflammation were reported. The downregulation of *Cebpb* may have led to the failure to regulate inflammation in the present study. Interestingly, *Lyz2* was the only gene that was upregulated in fibroblasts. *Lyz2* (lysozyme) encodes an enzyme with antimicrobial properties that plays a vital role in the innate immune response [52]. The upregulation of *Lyz2* in fibroblasts suggests enhanced antimicrobial activity within these cells, potentially

in response to prolonged exposure to microbial threats owing to the slow healing process. This upregulation could serve as a defence mechanism against infection or prolonged inflammation, which is especially important when the normal progression of wound healing is hindered. Noticeably, *lyz2* was also upregulated in macrophages, dendritic cells and neutrophils, immune cells critical for pathogen clearance and inflammatory regulation in wound healing. This shared upregulation across immune and stromal cell types may reflect a coordinated host response to persistent microbial threats in impaired wound healing environments. While immune cell recruitment appears compromised due to chemokine downregulation, the increased expression of *lyz2* could represent an alternative protective strategy to counteract potential infections. The balance between compromised immune recruitment and enhanced antimicrobial activity is crucial for wound healing. Therefore, this needs to be investigated further in future studies.

The presence of fibroblasts, endothelial cells, and erythroid cells in wound dressings may reflect mechanical shedding rather than direct biological responses within the wound. This raises the question of whether these cells are undergoing anoikis, a form of programmed cell death triggered when cells lose attachment to the extracellular matrix [53]. Anoikis serves as a protective mechanism, preventing detached cells from adhering to an abnormal environment [53]. Studies have shown that high glucose conditions can promote endothelial cell detachment and anoikis, which may contribute to increased cell shedding in diabetic wounds [54]. In the current study, we observed downregulation of several anoikis-related genes within specific cell clusters, including *Bcl3*, *Cebpb*, *Macl1*, *Thbs1*, *Ptgs2*, *Plaur*, *Fas*, *Cflar* and *Sbdbp*, which were downregulated, and *Vim*, *S100a4*, which were upregulated. This suggests that anoikis may not be the primary mechanism of cell loss in wound fluid. Instead, these cells may be sloughed off as part of extracellular matrix degradation, oxidative stress or mechanical disruption of tissue. The relationship between anoikis and cell shedding in wound healing remains unclear, and further studies are needed to determine whether the cells found in wound fluid undergo anoikis-driven apoptosis or are simply displaced into the dressing.

4.1 | Limitations

The genes identified in this study play roles in critical processes such as cell motility and immune responses, which are key to effective wound healing. However, the specific roles of these genes in wound healing have not been well documented, indicating a substantial area for further research. Investigating how these genes affect wound healing could lead to the identification of novel therapeutic targets. We used a small sample size due to the cost and feasibility. Nonetheless, this represents an initial screening step, and the potential of these biomarkers must be validated through further in vitro and in vivo studies. As the first dataset was derived from wound fluid, there were no existing comparable datasets for validation; in future studies, datasets from additional wound models or clinical wound fluid samples would help assess its reproducibility.

While some of our models did not exhibit significant delays in wound healing by PWD3, likely due to the short observation period, they are well-established models of delayed wound healing, ensuring the reliability of our findings. However, it is important to note that the wound models used in this study do not fully replicate human chronic, non-healing wounds. As such, the implications of our findings for human chronic ulcers require further validation. A key limitation of this study is the potential discrepancy between wound fluid cell populations and the actual wound bed environment. Although wound fluid provides a non-invasive and clinically feasible method for biomarker discovery, it may not fully represent all cellular components within the wound tissue. Especially for adherent cells, such as keratinocytes and resident fibroblasts, these may be underrepresented in wound fluid, as they primarily reside within the extracellular matrix and may not readily slough off into exudate. This could influence the detection of certain biomarkers and limit the ability to fully characterise the cellular dynamics within hard-to-heal wounds. Future studies should aim to compare wound fluid-derived cells with those obtained from tissue biopsies to further validate these findings. Some low-viability cells may die during cell processing and preparation of the library for RNA-seq, which may cause a possible lack of information on those cells that died during the process in the wound fluid. Additionally, cell viability in wound fluid may be influenced by various clinical conditions, including the type of wound dressing used (e.g., silver-containing dressings), environmental factors and the transition from the clinical setting to the laboratory. These factors could impact the interpretability of the wound fluid samples. Future clinical validation studies should consider these potential influences and validate findings in chronic wound fluid samples from patients.

4.2 | Future Implementation

This study explored the shared dysregulated genes in three representative hard-to-heal wound models using scRNA-seq and bioinformatics methods. Whether these biomarkers can serve as predictive indicators for risk screening and their potential predictive accuracy needs to be further validated. To strengthen the clinical applicability of these findings, future studies will focus on further expanding to patient-derived wound samples to assess biomarker consistency in human chronic wounds. Further elucidation of the mechanisms and possible related pathways underlying the relationship between these genes and hard-to-heal wounds is essential for the development of new predictive tools and intervention targets for clinical use. With these biomarkers, non-invasive screening tools for daily monitoring and timely treatment can be developed.

5 | Conclusion

To our knowledge, this is the first study to conduct scRNA-seq on cells extracted from discarded wound dressings. By analysing the transcriptomes of individual cells, we identified and quantified the different cell types present in the wound fluid. Upregulation of cell cycle cellular senescence-related genes and downregulation of immune response regulation were observed in the hard-to-heal wound group. Our study conducted scRNA-seq on wound fluid cells, which could provide a comprehensive, high-resolution view of the wound

environment, providing a deeper understanding of wound biology and potentially paving the way for more effective wound care strategies.

Author Contributions

Q.Q., D.H. and G.N. designed the study. Q.Q., D.H., C.T. and S.T. conducted experiments. Q.Q. analysed the results and wrote the manuscript. G.N. supervised the data analyses and data interpretation and revised the manuscript. S.N. and M.K. provided supervision on bioinformatic analyses and result interpretation. All authors reviewed and approved the manuscript.

Acknowledgements

This study was supported by the Fusion-Oriented Research for Disruptive Science and Technology (FOREST) of the Japan Science and Technology Agency (Grant JPMJFR205H), Japan Society for the Promotion of Science (JSPS) KAKENHI (Grant Nos. 23KJ0482, 23H00547) and the Research Support Project for Life Science and Drug Discovery (Basis for Supporting Innovative Drug Discovery and Life Science Research (BINDS)) from AMED (Grant JP23ama121016).

Conflicts of Interest

The authors declare no conflicts of interest.

Data Availability Statement

The data that support the findings of this study are available from the corresponding author upon reasonable request.

References

1. R. G. Frykberg and J. Banks, "Challenges in the Treatment of Chronic Wounds," *Advances in Wound Care* 4 (2015): 560–582.

2. C. K. Sen, G. M. Gordillo, S. Roy, et al., "Human Skin Wounds: A Major and Snowballing Threat to Public Health and the Economy," *Wound Repair and Regeneration* 17 (2009): 763–771.

3. D. Drgac and R. Himmelsbach, "Acts of Negotiation: Toward a Grounded Theory of Nursing Practice in Chronic Wound Care in Austria," *BMC Health Services Research* 23 (2023): 1–12.

4. B. Chan, S. Cadarette, W. Wodchis, J. Wong, N. Mittmann, and M. Krahn, "Cost-of-Illness Studies in Chronic Ulcers: A Systematic Review," *Journal of Wound Care* 26 (2017): S4–S14.

5. F. M. Davis, A. Kimball, A. Boniakowski, and K. Gallagher, "Dysfunctional Wound Healing in Diabetic Foot Ulcers: New Crossroads," *Current Diabetes Reports* 18 (2018): 2.

6. N. X. Landén, D. Li, and M. Ståhle, "Transition From Inflammation to Proliferation: A Critical Step During Wound Healing," *Cellular and Molecular Life Sciences* 73 (2016): 3861–3885.

7. S. Guo and L. A. DiPietro, "Factors Affecting Wound Healing," *Journal of Dental Research* 89 (2010): 219–229.

8. A. Selva Olid, I. Solà, L. A. Barajas-Nava, O. D. Gianneo, X. Bonfill Cosp, and B. A. Lipsky, "Systemic Antibiotics for Treating Diabetic Foot Infections," *Cochrane Database of Systematic Reviews* 2015 (2015): CD009061.

9. S. Ramsay, L. Cowan, J. M. Davidson, L. Nanney, and G. Schultz, "Wound Samples: Moving Towards a Standardised Method of Collection and Analysis," *International Wound Journal* 13 (2016): 880–891.

10. Y. Wang, T. Shao, J. Wang, et al., "An Update on Potential Biomarkers for Diagnosing Diabetic Foot Ulcer at Early Stage," *Biomedicine & Pharmacotherapy* 133 (2021): 110991.

11. H. N. Wilkinson and M. J. Hardman, "Wound Healing: Cellular Mechanisms and Pathological Outcomes," *Open Biology* 10 (2020): 200223.

12. S. Barrientos, O. Stojadinovic, M. S. Golinko, H. Brem, and M. Tomic-Canic, "Growth Factors and Cytokines in Wound Healing," *Wound Repair and Regeneration* 16 (2008): 585–601.

13. J. Y. Li, Z. J. Wang, A. P. Deng, and Y. M. Li, "ENA-78 Is a Novel Predictor of Wound Healing in Patients With Diabetic Foot Ulcers," *Journal Diabetes Research* 2019 (2019): 6–8.

14. X. Wang, J. Li, Z. Wang, and A. Deng, "Wound Exudate CXCL6: A Potential Biomarker for Wound Healing of Diabetic Foot Ulcers," *Biomarkers in Medicine* 13 (2019): 167–174.

15. I. R. Botusan, V. G. Sunkari, O. Savu, et al., "Stabilization of HIF-1α Is Critical to Improve Wound Healing in Diabetic Mice," *Proceedings of the National Academy of Sciences of the United States of America* 105 (2008): 19426–19431.

16. F. Ozsolak and P. M. Milos, "RNA Sequencing: Advances, Challenges and Opportunities," *Nature Reviews. Genetics* 12 (2011): 87–98.

17. G. Chen, B. Ning, and T. Shi, "Single-Cell RNA-Seq Technologies and Related Computational Data Analysis," *Frontiers in Genetics* 10 (2019): 1–13.

18. A. K. Shalek and M. Benson, "Single-Cell Analyses to Tailor Treatments," *Science Translational Medicine* 9 (2017): 1–4.

19. M. Januszyk, K. Chen, D. Henn, et al., "Characterization of Diabetic and Non-Diabetic Foot Ulcers Using Single-Cell RNA-Sequencing," *Micromachines* 11 (2020): 815.

20. C. F. Guerrero-Juarez, P. H. Dedhia, S. Jin, et al., "Single-Cell Analysis Reveals Fibroblast Heterogeneity and Myeloid-Derived Adipocyte Progenitors in Murine Skin Wounds," *Nature Communications* 10 (2019): 1–17.

21. G. Theocharidis, D. Baltzis, M. Roustit, et al., "Integrated Skin Transcriptomics and Serum Multiplex Assays Reveal Novel Mechanisms of Wound Healing in Diabetic Foot Ulcers," *Diabetes* 69 (2020): 2157–2169.

22. G. Theocharidis, B. E. Thomas, D. Sarkar, et al., "Single Cell Transcriptomic Landscape of Diabetic Foot Ulcers," *Nature Communications* 13 (2022): 181.

23. M. W. Löffler, H. Schuster, S. Bühler, and S. Beckert, "Wound Fluid in Diabetic Foot Ulceration: More Than Just an Undefined Soup?," *International Journal of Lower Extremity Wounds* 12 (2013): 113–129.

24. K. F. Cutting, "Wound Exudate: Composition and Functions," *British Journal of Community Nursing* 8 (2003): S4–S9.

25. I. Fuentes, C. Guttmann-Gruber, B. Tockner, et al., "Cells From Discarded Dressings Differentiate Chronic From Acute Wounds in Patients With Epidermolysis Bullosa," *Scientific Reports* 10 (2020): 1–10.

26. Q. Qin, D. Haba, C. Takizawa, et al., "A Method for Harvesting Viable Cells From Wound Dressings," *Experimental Dermatology* 32 (2023): 1521–1530.

27. A. Stachura, I. Khanna, P. Krysiak, W. Paskal, and P. Włodarski, "Wound Healing Impairment in Type 2 Diabetes Model of Leptin-Deficient Mice—A Mechanistic Systematic Review," *International Journal of Molecular Sciences* 23 (2022): 8621.

28. R. Crompton, H. Williams, D. Ansell, et al., "Oestrogen Promotes Healing in a Bacterial LPS Model of Delayed Cutaneous Wound Repair," *Laboratory Investigation* 96 (2016): 439–449.

29. K. A. Hwang, B. R. Yi, and K. C. Choi, "Molecular Mechanisms and In Vivo Mouse Models of Skin Aging Associated With Dermal Matrix Alterations," *Laboratory Animal Research* 27 (2011): 1–8.

30. G. X. Y. Zheng, J. M. Terry, P. Belgrader, et al., "Massively Parallel Digital Transcriptional Profiling of Single Cells," *Nature Communications* 8 (2017): 14049.

31. Y. Hao, S. Hao, E. Andersen-Nissen, et al., "Integrated Analysis of Multimodal Single-Cell Data," *Cell* 184 (2021): 3573–3587.

32. C. Hu, T. Li, Y. Xu, et al., "CellMarker 2.0: An Updated Database of Manually Curated Cell Markers in Human/Mouse and Web Tools Based on scRNA-Seq Data," *Nucleic Acids Research* 51 (2023): D870–D876.

33. O. Franzén, L. M. Gan, and J. L. M. Björkegren, "PanglaoDB: A Web Server for Exploration of Mouse and Human Single-Cell RNA Sequencing Data," *Database* 2019 (2019): 1–9.

34. X. Shao, J. Liao, X. Lu, R. Xue, N. Ai, and X. Fan, "scCATCH: Automatic Annotation on Cell Types of Clusters From Single-Cell RNA Sequencing Data," *iScience* 23 (2020): 100882.

35. M. Asada, G. Nakagami, T. Minematsu, et al., "Novel Biomarkers for the Detection of Wound Infection by Wound Fluid RT-PCR in Rats," *Experimental Dermatology* 21 (2012): 118–122.

36. D. R. Yager, R. A. Kulina, and L. A. Gilman, "Wound Fluids: A Window Into the Wound Environment?," *International Journal of Lower Extremity Wounds* 6 (2007): 262–272.

37. C. Chen, J. Peng, S. Ma, et al., "Ribosomal Protein S26 Serves as a Checkpoint of T-Cell Survival and Homeostasis in a p53-Dependent Manner," *Cellular & Molecular Immunology* 18 (2021): 1844–1846.

38. L. Daftuar, Y. Zhu, X. Jacq, and C. Prives, "Ribosomal Proteins RPL37, RPS15 and RPS20 Regulate the Mdm2-p53-MdmX Network," *PLoS One* 8 (2013): e68667.

39. S. Kathju, L. Satish, C. Rabik, et al., "Identification of Differentially Expressed Genes in Scarless Wound Healing Utilizing Polymerase Chain Reaction—Suppression Subtractive Hybridization," *Wound Repair and Regeneration* 14 (2006): 413–420.

40. F. Lessard, S. Igelmann, C. Trahan, et al., "Senescence-Associated Ribosome Biogenesis Defects Contributes to Cell Cycle Arrest Through the Rb Pathway," *Nature Cell Biology* 20 (2018): 789–799.

41. A. Ridiandries, J. Tan, and C. Bursill, "The Role of Chemokines in Wound Healing," *International Journal of Molecular Sciences* 19 (2018): 3217.

42. Y. Cao, Z. Chen, Z. Qin, K. Qian, T. Liu, and Y. Zhang, "CDKN2AIP-Induced Cell Senescence and Apoptosis of Testicular Seminoma Are Associated With CARM1 and eIF4β," *Acta Biochimica et Biophysica Sinica* 54 (2022): 604–614.

43. J. Bartkova, B. Grøn, E. Dabelsteen, and J. Bartek, "Cell-Cycle Regulatory Proteins in Human Wound Healing," *Archives of Oral Biology* 48 (2003): 125–132.

44. H. Huy, H. Y. Song, M. J. Kim, et al., "TXNIP Regulates AKT-Mediated Cellular Senescence by Direct Interaction Under Glucose-Mediated Metabolic Stress," *Aging Cell* 17 (2018): e12836.

45. Y. E. Hadisaputri, T. Miyazaki, T. Yokobori, et al., "TNFAIP3 Overexpression Is an Independent Factor for Poor Survival in Esophageal Squamous Cell Carcinoma," *International Journal of Oncology* 50 (2017): 1002–1010.

46. H. N. Wilkinson and M. J. Hardman, "Senescence in Wound Repair: Emerging Strategies to Target Chronic Healing Wounds," *Frontiers in Cell and Development Biology* 8 (2020): 773.

47. E. G. Lee, D. L. Boone, S. Chai, et al., "Failure to Regulate TNF-Induced NF-κB and Cell Death Responses in A20-Deficient Mice," *Science* 289, no. 5488 (2000): 2350–2354.

48. C. Kerkhoff, A. Voss, T. E. Scholzen, M. M. Averill, K. S. Zänker, and K. E. Bornfeldt, "Novel Insights Into the Role of S100A8/A9 in Skin Biology," *Experimental Dermatology* 21 (2012): 822–826.

49. M. Benedyk, C. Sopalla, W. Nacken, et al., "HaCaT Keratinocytes Overexpressing the S100 Proteins S100A8 and S100A9 Show Increased NADPH Oxidase and NF-κB Activities," *Journal of Investigative Dermatology* 127 (2007): 2001–2011.

50. Q. Ren, Z. Liu, L. Wu, et al., "C/EBPβ: The Structure, Regulation, and Its Roles in Inflammation-Related Diseases," *Biomedicine & Pharmacotherapy* 169 (2023): 115938.

51. V. E. Dunlock, "Tetraspanin CD53: An Overlooked Regulator of Immune Cell Function," *Medical Microbiology and Immunology* 209 (2020): 545–552.

52. L. Jiang, Y. Li, L. Wang, et al., "Recent Insights Into the Prognostic and Therapeutic Applications of Lysozymes," *Frontiers in Pharmacology* 12 (2021): 767642.

53. A. P. Gilmore, "Anoikis," *Cell Death and Differentiation* 12, no. 2 (2005): 1473–1477.

54. D. Dobler, N. Ahmed, L. Song, K. E. Eboigbodin, and P. J. Thornalley, "Increased Dicarbonyl Metabolism in Endothelial Cells in Hyperglycemia Induces Anoikis and Impairs Angiogenesis by RGD and GFOGER Motif Modification," *Diabetes* 55, no. 7 (2006): 1961–1969.

Supporting Information

Additional supporting information can be found online in the Supporting Information section.